BC10 O-North multi-attributes seismic inversion for saturation changes using ML

Yang Xue[1], Carlos Nieto[2], Kanglin Wang[1], [1]Shell International Exploration and Production Inc., [2]Shell Brasil Petróleo Ltda

Abstract

Time lapse (4D) seismic is widely deployed in offshore operations to monitor reservoir changes, especially those utilizing improved oil recovery methods including water flooding. But its value for well and reservoir management (WRM) is not fully realized due to the long cycle time required transferring the 4D seismic into reservoir property changes, such as water/gas saturation changes and pressure changes. To shorten the cycle time, we designed a machine learning based agile workflow to invert for reservoir property changes directly from a variety of 4D seismic attribute maps and reservoir static property maps. We use reservoir simulation, calibrated rock physics model and the real seismic data well tied wavelet to generate synthetic 4D seismic data and their attribute maps. As the reservoir property changes are related not only to the 4D attribute maps, but also to the reservoir static parameters, each training dataset is composed of multi-4D attributes and static parameters from reservoir simulation as input, and the reservoir property changes from the reservoir simulator as output. A shallow neural net (NNet) is applied to train on the synthetic datasets demonstrating satisfactory convergence within a few minutes, allowing prediction of property changes from the real 4D seismic attribute maps with seconds of time.

This ML based agile workflow is applied to BC10 O-North field to predict water and gas saturation changes (*dSw and dSg*) simultaneously. The turnaround time can be reduced from weeks to days, allowing early engagements with reservoir engineers to enhance integration and removing a deterrent to the acquisition of frequent 4D surveys.

Introduction

When interpreting 4D seismic signals, people often have to face the trade-off between qualitative and quantitative approaches, e.g., normalized root mean square amplitude changes, *NdRMS*, or to apply inversion methods to quantify reservoir property changes by matching the seismic wiggles of baseline and monitor surveys. Qualitative interpretation of 4D attribute maps detects where changes have occurred based on observed effects and their direction (hardening or softening). However, the amount of change cannot be quantified. 4D inversion can quantify reservoir property changes and provide uncertainty estimates. However, it requires sophisticated inversion process. Consequently, the turnaround time can extend to weeks or months while the business impact fades.

To fill the gap between qualitative interpretation of 4D attribute maps and 4D inversion, several ML and DL based workflows (Cao et al. 2017, Xue et al. 2019, Côrte et al. 2020) are used to predict the maps of reservoir property changes. The ideas are similar in a way that using machine-learning model trained from the synthetic data to replace the nonlinear physics models (rock and fluids models and calculation of seismic reflection coefficients). After a successful training, the non-linear inversion problem is then transferred to a machine learning based forward model, thus enable the prediction in a very quick time. Previous study from Xue et. al. (2018) using only one attribute (*NdRMS* or *dRMS*) to invert for *dSw* and *dSg* separately assuming there is no overlap between *dSw* and *dSg*. In this paper, we extend the workflow for a simultaneous inversion of *dSw* and *dSg* by adding multi-attributes from 4D seismic data.

The non-uniqueness remains one of the biggest challenges for simultaneous inversion of reservoir property changes, i.e. softening signal may come from water saturation decrease, or from gas saturation increase or from pressure increase, or from a combination of these effects. Using reservoir properties populated from reservoir simulations as the training datasets can provide constrains to such non-uniqueness as the physical relationships between these properties are embedded and unrealistic scenarios are excluded. Adding a variety of 4D attributes as input further helps to reduce the degree of freedom. In the end, the predicted property changes together with their uncertainties will provide quantitative insights to support reservoir development and operation decisions.

Method

The workflow of multi-attributes seismic inversion for saturation changes uses ML approach with three steps: 1) generate the synthetic training datasets; 2) build, train and test the NNet; 3) predict the reservoir property changes on the real data.

The first step is to generate the synthetic 4D seismic responses. Reservoir model simulated property changes, calibrated rock physics model and real seismic well tied wavelet are applied to generate the synthetic 4D seismic wiggles. Then, a variety of seismic attribute maps (i.e. listed in Table 1) were calculated within the gate of reservoir layer. Those synthetic 4D attribute maps together with the static properties (including net-to-gross, porosity and saturation baseline) and reservoir simulated

property changes compose the synthetic database for the next step.

4D attributes	Description
dRMS	Difference of root mean square amplitude between baseline and monitor
SNADiff	Absolute value of summation of negative amplitude of seismic difference
SPADiff	Absolute value of summation of positive amplitude of seismic difference
dSNA	Difference of summation of negative amplitude between baseline and monitor
dSPA	Difference of summation of positive amplitude between baseline and monitor

Table 1: List of 4D attributes used and how they are calculated.

The second step is to build, train and test the ML model on the synthetic datasets. The total synthetic datasets are split into two parts, one for training and the rest for testing. Here we use a shallow NNet (with only two hidden layers) as our ML model, which already provided a satisfactory convergence in a very quick time.

The last step is to use the trained NNet to predict the *dSw* and *dSg* simultaneously with the synthetic 4D seismic attribute maps replaced by the real 4D attribute maps. For the uncertainty analysis in a practical way, we repeat the workflow from step 1 to 3 multiple times, calculate the standard deviation of the predictions and compare with the mean average.

Examples – BC10 O-North background

The O-North field located within the BC10 license, northern Campos Basin – Brasil, is a large and very flat structure conformed by amalgamated channelized turbidites with high net-to-gross within the main channel body. This heavy oil field is produced by waterflood recovery using 12 long horizontal wells (8 producers and 4 injectors); all wells with high productivity and injectivity. The initial reservoir pressure is close to bubble point. Given the small pressure range and the high viscosity of the oil, coning, cusping and fingering of water is observed in 4D seismic monitor surveys. Injectivity and productivity rates are optimized to manage the waterflood sweep, gas-oil-ratio and reservoir pressure, using 4D seismic data. Infill drilling opportunities are also defined using 4D seismic data. Given the importance of 4D for the development of this field, a permanent reservoir monitoring system was installed in 2013, known as LoFS: Life of Field Seismic, which consists of 4-components sensors deployed along Ocean Bottom Cables connected to the FPSO and provides the opportunity to acquire frequent reservoir monitoring surveys. The BC-10 Asset has acquired a baseline survey in 2013, and 5 monitor surveys, last one in January 2020, which was processed using the most recent 4D joint Kirchhoff LSM workflow yielding 3D and 4D partial angle stack volumes as well as pre-stack gathers.

The team is working towards two key projects in O-North: (1) Waterflood Optimization, the first step towards the Integrated Ramp-Up Plan, and (2) Polymer Flooding injection pilot to increase water viscosity which would lead to stable oil displacement, effectively reducing fingering and increasing sweep efficiency (increase oil recovery and lower water cut). The understanding of vertical permeability and preferential flow paths of the reservoir will provide valuable knowledge for these two key projects.

To understand the relation between the saturation vs. pressure effects in the reservoir the team relied on qualitative 4D seismic interpretation, as well as quantitative approach ML inversion, object of this study. 4D AvA intercept and gradient analysis is also included to understand the behavior among the 4 injectors, and their correlation with the injectivity rates. The results will be integrated/included to the model via 4D QSRM (quantitative seismic reservoir modeling) in due time, once resources become available.

Examples – BC10 O-North ML inversion results

Following **the first step** of the workflow, we use reservoir simulation model, calibrated rock physics model and real seismic well tied wavelet to generate synthetic 4D seismic data and their 4D attribute maps (figure 1). Strong correlation is observed between 4D attribute maps and *dSw and dSg* maps: i.e. *SNADiff* focusing on the softening signal is primary dominated by gas saturation increase, thus has a similar pattern as the *dSg*, while *SPADiff* focusing on the hardening signal is strongly correlated with *dSw*. *SNADiff* and *SPADiff* may help for a joined inversion of *dSw and dSg* but the sign information is missed from these two attributes. Other 4D attributes in the table 1, such as *dRMS* and *dSNA* have the correct sign information, which will fill the drawback from *SNADiff* and *SPADiff*.

In the second step, we built a two-hidden layer NNet with the input composed of the 4D attribute maps calculated from the step one and the maps of static properties from reservoir model, and the reservoir simulated *dSw* and *dSg* as output. The synthetic datasets were split equally. Half of them are used for training and the rest for testing. R2 score (the square of the correlation coefficient between the true outcomes and the predicted values) is commonly used for the regression accuracy assessment, normally ranges from 0 to 1 with 0 meaning no correlation and 1 meaning the exact same. In this test, we achieved a satisfactory prediction just in a few minutes of CPU time, with the R2 score of 0.85 for *dSw* and 0.94 for *dSg*. The residuals between the predicted *dSw & dSg* and the ground truth (synthetic *dSw & dSg*) is shown in the figure 2. The average residuals for *dSw* is c.a 0.002 with a standard deviation of 0.03 and for *dSg* is c.a. 0.00001 with a standard deviation of 0.0008. We also noticed that the residuals are mostly located at the overlapping area where both *dSw* and *dSg* are present, i.e. near the center and southeastern producers (wells in black), where machine tends to have a little overestimated for *dSg* and underestimated for *dSw*.

After the NNet was trained, the real 4D seismic attributes maps (figure 3) were substituted for the synthetic 4D

seismic attributes maps **in the last step**. To quantify the robustness of estimation, we repeated the workflow 20 times and calculated the mean average of *dSw & dSg* maps and their standard deviation maps accordingly (figure 4). The standard deviation for *dSw* is below 0.08 and for *dSg* is below 0.01. The uncertainty of *dSw* (figure 4c) is larger along the injectors where the magnitude of *dSw* is larger too. The uncertainty of *dSg* (figure 4d) is larger around the producers where *dSw* and *dSg* may overlap. By comparing the average and standard deviation for each variable, we can locate where we have robust estimation and where we have large uncertainty. For example, the producer at the southwest corner (shown in black) has a relatively large standard deviation of *dSg*, which almost reaches the same magnitude as the average, indicating the *dSg* estimation may not be robust at that location.

Another factor that also contributes to the uncertainties is the unknown pressure change (*dP*). Simultaneous inversion for both pressure changes and saturation changes is quite challenging without shear wave data. In this example as pressure is well maintained at BC10 O-North, we assume that the saturation changes are the dominant contributors for the 4D signal and pressure effect is secondary. If significant pressure changes are present in the surveillance data, we can add *dP* from reservoir simulation as one of the inputs to adjust the pressure impact.

Conclusions and discussion

A ML based agile workflow using multi-attributes of 4D seismic for simultaneous inversion of *dSw* and *dSg* is designed and tested to fill the gaps between qualitative interpretation of 4D attribute maps and 4D inversion of seismic wiggles and to deliver a solution in a very quick time. A good prediction of saturation changes using synthetic data is demonstrated, with a slightly narrower uncertainty for *dSg* than for *dSw* as the 4D seismic amplitude change is more sensitive to *dSg*. We also applied this workflow to the real dataset (BC10 O-North) to estimate water/gas saturation changes from a combination of multi-4D attributes and the static properties from the reservoir model.

One of the major uncertainties for simultaneous inversion of reservoir property changes comes from the non-uniqueness, meaning multiple combinations of inversion results may lead to the same 4D response. Thus, a good starting point with relevant training datasets is essential for a satisfactory convergence and robust prediction. Here we use physics based synthetic data with reservoir model simulation, rock physics model and real seismic well tied wavelet, to construct a reasonable framework for training. We also accessed the robustness of prediction by running the workflow multiple times. The mean average and the standard deviation of the predictions can be used for uncertainty analysis. Additionally, if multiple reservoir models with different static parameters settings are available, the sensitivity of the inversion can be accessed through a similar strategy: repeat the workflow with different static models and analyze the variance of the predictions. The estimated saturation changes and their uncertainties can then be used to provide key geophysical

input to timely analyze injection efficiency, update the reservoir model, and support decisions on the water flood optimization. The efficiency advantage is more substantial for multiple repeated 4D seismic surveys.

References

Cao, J., and B. Ray, 2017. Time-lapse reservoir property change estimation from seismic using machine learning: The Leading Edge, volume 36, issue 3, 234-238, doi: 10.1190/tle36030234.1.

Côrte, G., J. Dramsch, H. Amini and C. MacBeth, 2020. Deep neural network application for 4D seismic inversion to changes in pressure and saturation: optimizing the use of synthetic training datasets, Geophysical Prospecting, 68, 2164-2185

Xue, Y., M. Araujo, J. Lopez, K. Wang and G. Kumar, 2019. Machine learning to reduce cycle time for time-lapse seismic data into reservoir management, Interpretation, volume 7, issue 3, https://doi.org/10.1190/INT-2018-0206.1
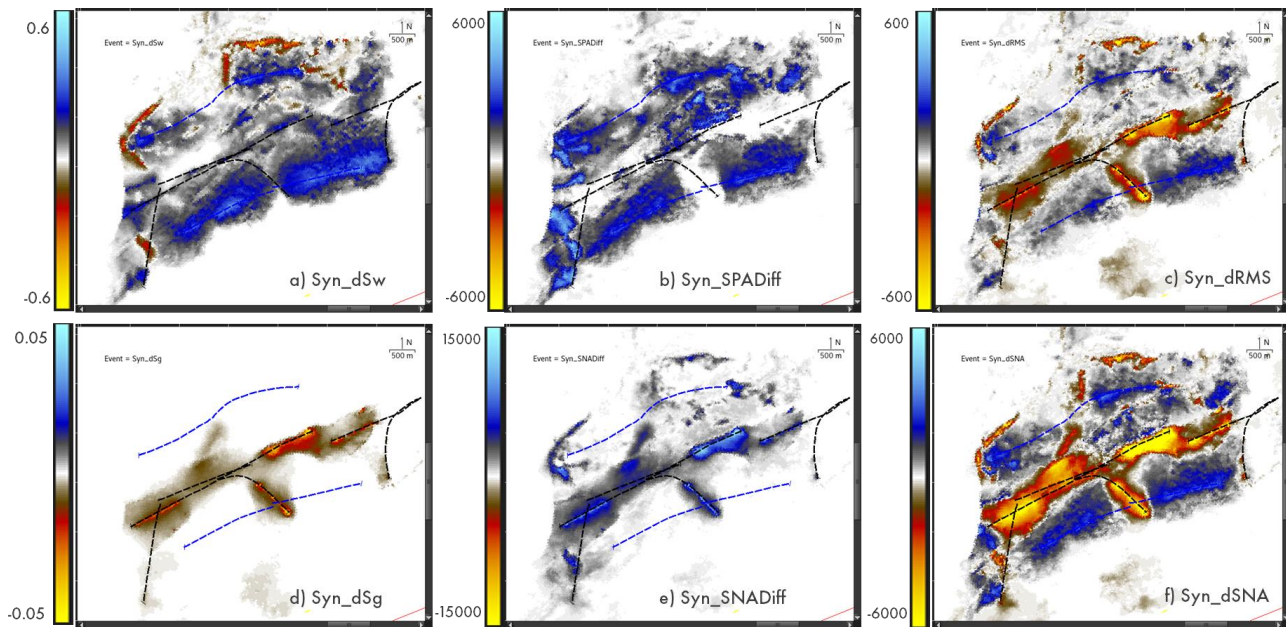
Figure 1: a) synthetic *dSw* map; b) synthetic *SPADiff* map; c) synthetic *dRMS* map; d) synthetic *dSg* map; e) synthetic *SNADiff* map; f) synthetic *dSNA* map. Gate used to calculate the 4D attribute map is from reservoir top to reservoir bottom.
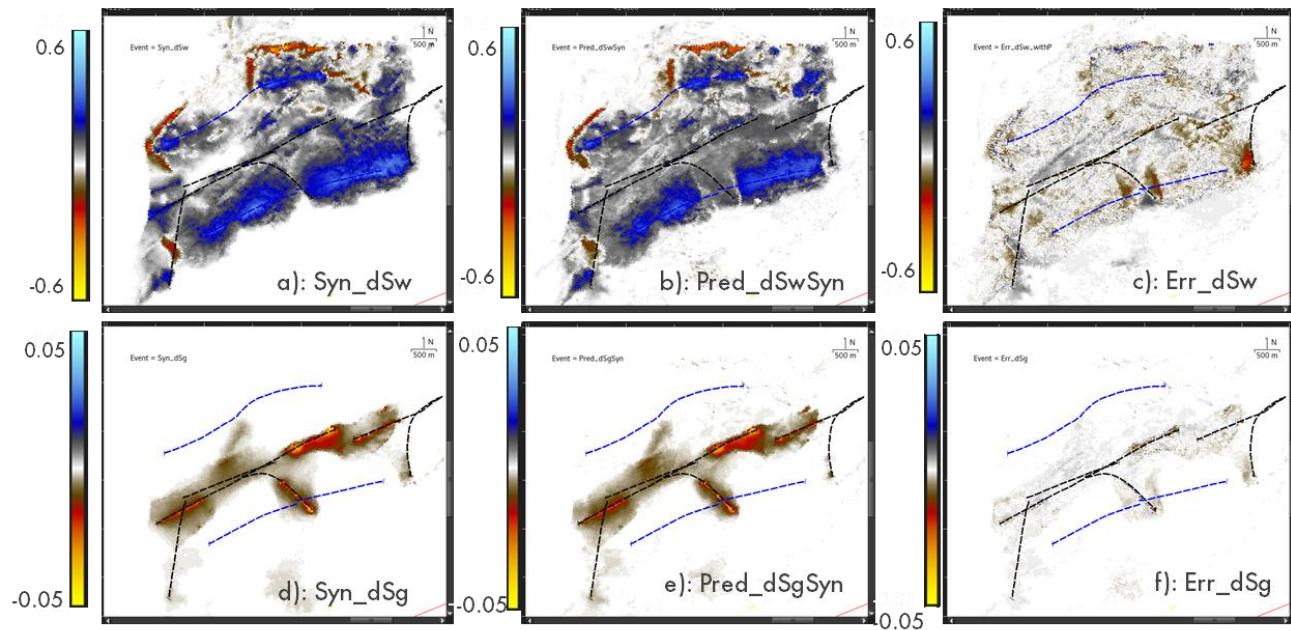
Figure 2: a) synthetic *dSw* map; b) predicted *dSw* map; c) difference of *dSw* map between predicted and the ground truth; d) synthetic *dSg* map; e) predicted *dSg* map; f) difference of *dSg* map between predicted and the ground truth.
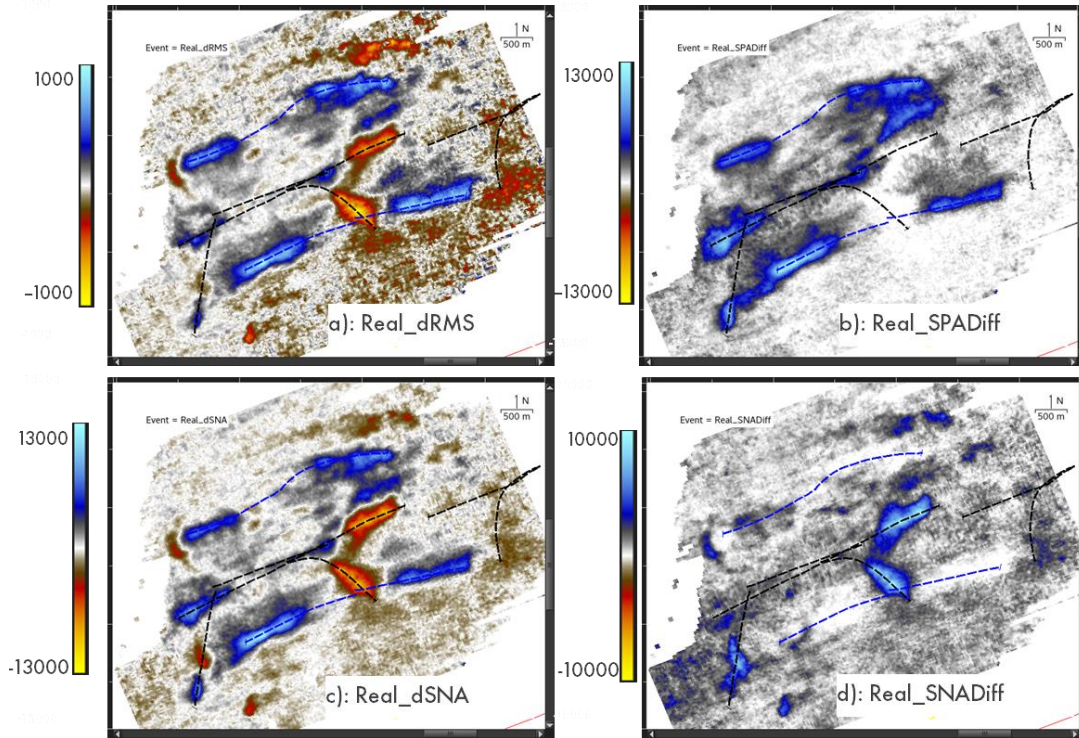
Figure 3: a) Real *dRMS* map; b) real *SPADiff* map; c) real *dSNA* map; d) real *SNADiff* map. Gate used to calculate the 4D attributes for real data is the same as applied in the synthetic data.
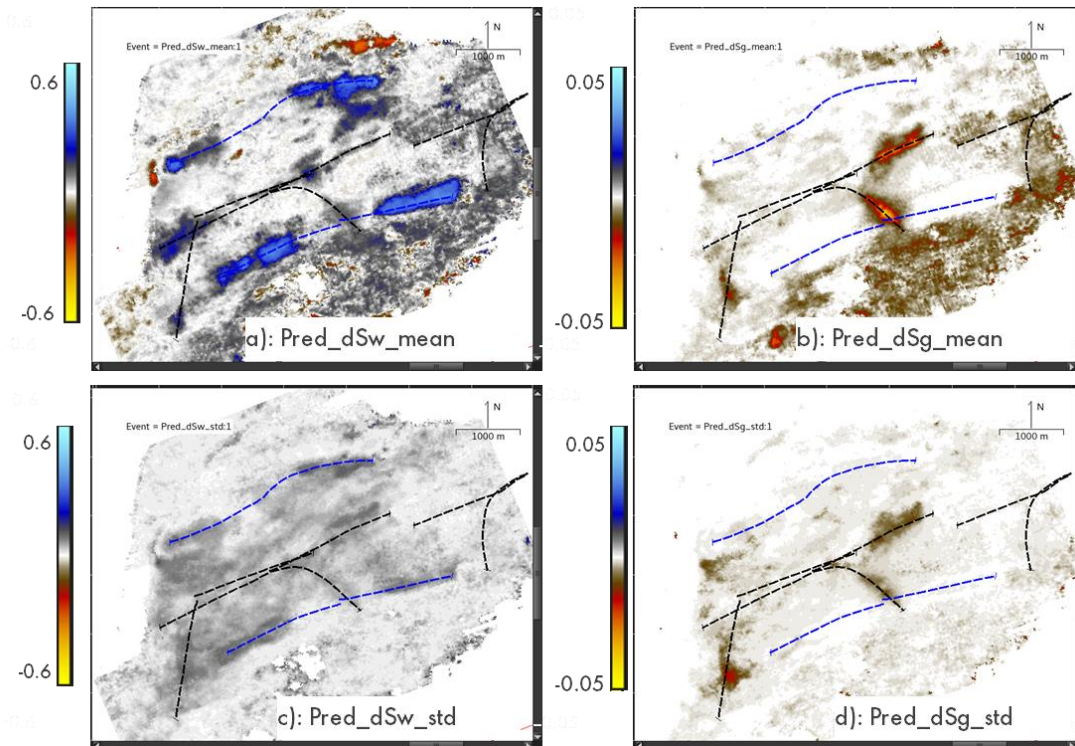
Figure 4: a) the mean average of predicted *dSw* maps from the 20 runs; b) the mean average of predicted *dSg* maps from the 20 runs; c) the standard deviation of *dSw* maps from the 20 runs; d) the standard deviation of *dSg* maps from the 20 runs.